scientific reports

Check for updates

OPEN

Integrative network pharmacology and experimental validation of anti-inflammatory triterpenoids from hawthorn leaves

Zhixing Liu & Jihua Liu✉

A network pharmacology approach was employed to identify key bioactive compounds and core targets in hawthorn leaves with potential anti-inflammatory properties. The predicted biological effects and underlying mechanisms were systematically validated through target enzyme activity evaluations, molecular docking simulations, LPS-induced inflammatory models in RAW264.7 macrophages, western blot and quantitative real-time PCR (qRT-PCR) analyses. Molecular docking studies revealed strong binding affinities of triterpenoids 99, 102, and 116 to SRC (Proto-Oncogene Tyrosine-Protein Kinase Src), a critical regulator of inflammatory signaling pathways. These interactions were further substantiated by enzymatic activity assays and macrophage-based inflammatory models. Notably, the triterpenoids showed strong anti-inflammatory properties by significantly reducing nitric oxide (NO) release and altering the expression of inflammatory genes in LPS-stimulated RAW264.7 macrophages. Among them, triterpenoid 99 demonstrated the most pronounced activity, primarily by downregulating SRC mRNA and protein expression. These findings provide compelling scientific evidence supporting the use of hawthorn leaves as a natural reservoir of anti-inflammatory agents, offering a strong foundation for future pharmacological and therapeutic developments.

Inflammation is a crucial bodily defense process against various harmful stimuli, marked by the attraction of immune cells, the release of inflammatory substances, and heightened vascular permeability. Effective inflammation management necessitates addressing the underlying causes and providing symptomatic relief. While acute inflammation is essential for pathogen elimination and tissue repair, persistent or chronic inflammation is implicated in the pathogenesis and progression of numerous diseases, including autoimmune disorders, cardiovascular diseases, metabolic syndromes such as diabetes, and various cancers[1,2]. Effective management of inflammation requires not only symptomatic relief but also targeted intervention in the underlying pathological mechanisms[1,2]. Currently, nonsteroidal anti-inflammatory drugs (NSAIDs) and steroidal anti-inflammatory drugs (SAIDs) are widely utilized for inflammation control due to their efficacy in inhibiting key inflammatory pathways[3]. However, long-term use of these pharmacological agents is often associated with severe adverse effects, including gastrointestinal ulceration, renal dysfunction, hypertension, and increased cardiovascular risks[3]. There is an urgent need for safer and more effective anti-inflammatory agents with minimal toxicity and superior therapeutic potential. Natural products have been valued for a long time as a valuable resource in the search for novel therapeutic agents. These compounds are frequently associated with favorable safety profiles and notable therapeutic efficacy[4]. Consequently, the identification of novel anti-inflammatory agents derived from natural sources, particularly those with minimal toxicity and broad therapeutic potential, remains a critical focus in the development of safer and more effective anti-inflammatory therapies.

Hawthorn (*Crataegus pinnatifida* Bunge.), a deciduous tree belonging to the *Rosaceae* family, has been extensively utilized in traditional medicine for its broad-spectrum therapeutic effects. Extracts derived from this species are widely incorporated into dietary supplements, functional foods, and pharmaceutical products[5]. The dried leaves of hawthorn are particularly rich in bioactive compounds, including flavonoids, phenolics and triterpenoids, which have a wide range of biological activities such as antioxidant, hypotensive, hypolipidemic and anti-inflammatory effects, making it a popular herbal medicine for phytotherapy and food applications[6,7]. For instance, ethanol extracts of hawthorn leaves have demonstrated significant anti-inflammatory and analgesic effects in animal models by reducing ear swelling and torsion responses[8]. Several bioactive compounds in hawthorn leaves have demonstrated promising anti-inflammatory potential. Flavonoids, such as poncirin have

College of Pharmaceutical Science, Jilin University, Changchun 130021, China. ✉email: liujh@jlu.edu.cn

been reported to exert antioxidant and anti-inflammatory effects by inhibiting oxidative stress, inflammatory mediators, and apoptosis pathways, offering potential cardioprotective benefits[9,10]. Furthermore, phenolic compounds, flavonoids, and proanthocyanidins in hawthorn leaf and flower tea have been shown to alleviate colitis by reducing myeloperoxidase and interleukin-1β levels while enhancing glutathione reductase and catalase activities[11]. Among the key bioactive constituents, triterpenoids have gained increasing attention for their significant anti-inflammatory activity. For example, hawthornic acid, a pentacyclic triterpenoid, has been shown to suppress LPS-induced inflammatory responses in RAW264.7 cells by inhibiting the activation and phosphorylation of the transcription factor STAT3[12]. Additionally, triterpenoids such as ursolic acid, commonly found in hawthorn, have been shown to modulate inflammatory responses through decreasing the mRNA expression levels of TNF-α, IL-1β, IL-6, COX-2, NO, and iNOS[13]. Despite promising evidence of the anti-inflammatory effects of hawthorn leaf triterpenoids, few studies have integrated network pharmacology with experimental validation to systematically elucidate their mechanisms of action.

In this study, network pharmacology was employed to predict the anti-inflammatory active components and potential molecular targets of hawthorn leaf compounds. The key interactions between these bioactive compounds and inflammation-related targets were validated through enzymatic activity assays and molecular docking analyses. The anti-inflammatory properties of the active ingredients were further examined using LPS-induced RAW264.7 macrophage models, combined with real-time PCR. The study aims to identify novel anti-inflammatory agents derived from hawthorn leaves and provide mechanistic insights into their action, thereby advancing the development of safer, more effective anti-inflammatory therapies.

Results and discussion

Network pharmacology analysis

To explore the anti-inflammatory potential of hawthorn leaf constituents, a network pharmacology approach was employed. The structural data of 116 identified chemical constituents were retrieved in SDF format from the PubChem database (https://pubchem.ncbi.nlm.nih.gov/). These molecular structures were then submitted to the PharmMapper server (http://www.lilab-ecust.cn/pharmmapper/) for target prediction, using a Norm Fit score threshold of ≥ 0.7 to ensure high-confidence predictions. After removing duplicates, 178 potential target proteins were identified. Inflammation-related targets were retrieved from the Gene Cards database (https://www.genecards.org/) using the keyword "inflammation," resulting in 1852 relevant targets (score > 2.73). By intersecting the hawthorn constituent targets with inflammation-related targets, 53 overlapping anti-inflammatory targets were identified (Fig. 1A).

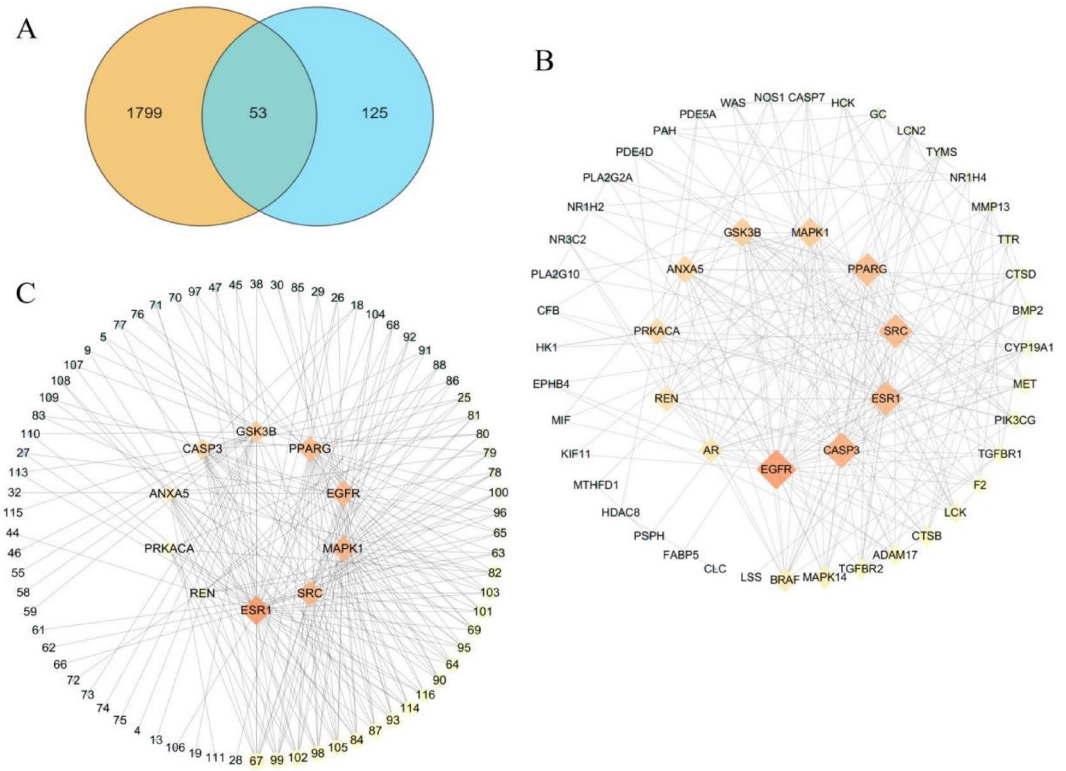

Fig. 1. Network pharmacology analysis.(**A**) Venn diagram showing the intersection of hawthorn leaf chemical composition-related targets and inflammation-related targets.(**B**) Protein–protein interaction (PPI) network of inflammation-related targets.(**C**) Network of hawthorn leaf chemical compounds and inflammation-related targets. Circular nodes represent chemical compounds, with node size indicating the number of interactions with target proteins. Diamond-shaped nodes represent target proteins.

The STRING database was utilized to construct a PPI network of the 53 targets. Core targets were identified based on topological metrics, including degree centrality, betweenness centrality, and closeness centrality. The ten most important targets were ranked as follows: Estrogen receptor (ESR1), Proto-oncogene tyrosine-protein kinase Src (SRC), Mitogen-activated protein kinase 1 (MAPK1), Epidermal growth factor receptor (EGFR), Peroxisome proliferator-activated receptor gamma (PPARG), Glycogen synthase kinase-3 beta (GSK3B), Caspase-3 (CASP3), Annexin A5 (ANXA5), cAMP-dependent protein kinase catalytic subunit alpha (PRKACA), and Renin (REN) (Fig. 1B).

A simplified chemical component-target interaction network was constructed using Cytoscape 3.9.1, integrating 116 chemical components with the 10 core inflammatory targets. The network demonstrated that hawthorn leaves exert anti-inflammatory effects through the synergistic interactions of multiple components and targets, reflecting their complex pharmacological mechanisms. Topological properties of the network were analyzed using the "Network Analyzer" function, with node size and color intensity representing Degree values. Larger and darker nodes indicated higher Degree values, signifying greater importance. ESR1, SRC, MAPK1, EGFR, and PPARG were the top five targets with the highest Degree values (Fig. 1C).

The top 10 chemical components, ranked by Degree values, were: 3β-glucopyranosyloxy-β-ionone (67), 2α,3α,19α-trihydroxyurs-12-en-28-oic acid (99), crataegolic acid (102), 3-β-O-acetyl ursolic acid (98), tortoside A (105), 18,19-seco,2α,3β-dihydroxy-19-oxo-urs-11,13(18)-dien-28-oic acid (84), linarionoside A (87), 10,11-dihydroxynerolidol (93), (+)−7R,8 S-5-methoxydihydrodehydroconiferyl alcohol (114), and oleanolic acid (116).

Notably, previous studies have shown that maslinic acid (hawthorn acid), a natural pentacyclic triterpenoid, exhibits protective effects against chronic inflammatory diseases in vivo and in vitro. These effects are attributed to its regulation of arachidonic acid metabolism, including the modulation of nuclear NF-κB, COX-2 expression, upstream protein kinase signaling, and phospholipase A2 activity. The identification of maslinic acid and other bioactive triterpenoids in our study aligns with these findings, further substantiating the predictive accuracy of network pharmacology in identifying active constituents and elucidating their mechanisms of action[14]. These results suggest that hawthorn leaf extracts may exert their anti-inflammatory effects via a multi-target, multi-pathway mode of action, characteristic of traditional herbal medicines. Further validation through experimental pharmacological assays, including molecular docking, and cellular assays, is warranted to confirm the therapeutic relevance of the identified compounds.

The 53 core anti-inflammatory targets of hawthorn leaves were subjected to Gene Ontology (GO) and Kyoto Encyclopedia of Genes and Genomes (KEGG) enrichment analyses using the DAVID database. GO analysis categorized the targets into three domains: Biological Process (BP), Cellular Component (CC), and Molecular Function (MF). KEGG analysis was conducted to predict the roles of these targets in cellular activities and to identify key protein pathways and interactions.

GO enrichment analysis identified a total of 264 pathways, distributed across 170 biological processes (BPs), 63 molecular functions (MFs), and 31 cellular components (CCs) (Fig. 2). In the BP domain, the most enriched pathways included signal transduction, phosphorylation, positive regulation of transcription by RNA polymerase II, and cell population proliferation. For MF, pathways such as protein binding, ATP binding, identical protein binding, and signaling receptor binding were highlighted. In the CC domain, core targets were associated with the cytosol, plasma membrane, nucleus, extracellular region, and cytoplasm (Fig. 3).

KEGG pathway enrichment analysis revealed that the 53 key anti-inflammatory targets were involved in critical pathways, including cancer-related pathways, metabolic pathways, the relaxin signaling pathway,

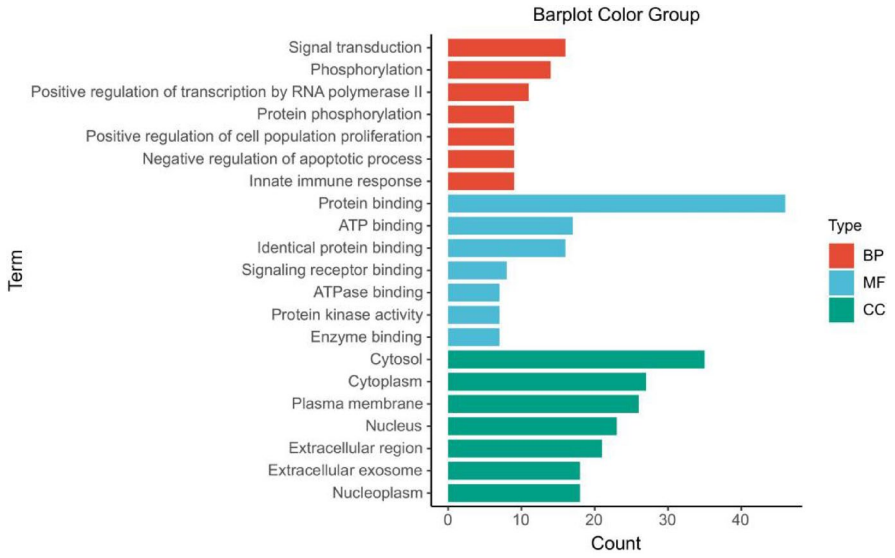

Fig. 2. GO analysis of target proteins, including BP, MF, and CC categories.

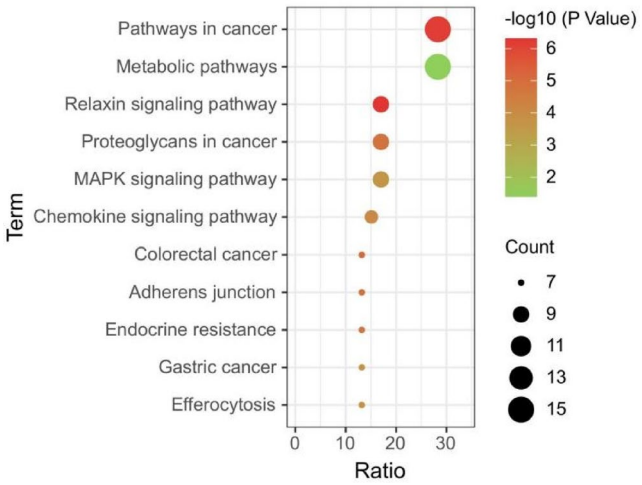

Fig. 3. KEGG pathway enrichment analysis of 53 target proteins.

proteoglycans in cancer, the MAPK signaling pathway, and the chemokine signaling pathway. These findings provide insights into the molecular mechanisms of hawthorn leaf compounds (Fig. 3).

Experimental validation of kinases

SRC is a critical non-receptor tyrosine kinase involved in cellular signaling pathways that regulate essential processes such as proliferation, migration, survival, and cytoskeletal reorganization. Its activation is closely linked to cancer, inflammation, and various physiological and pathological processes. In the context of inflammation, SRC plays a pivotal role by modulating immune cell activation, inflammatory responses, and tissue damage through multiple signaling pathways. SRC is highly expressed in immune cells, including macrophages, T cells, B cells, and dendritic cells, where it mediates signaling via its tyrosine kinase activity in response to pathogenic infections or damage signals[15]. SRC inhibition exerts broad anti-inflammatory effects by modulating key signaling pathways involved in immune responses. It suppresses NF-κB activation by preventing IκB-α degradation, thereby reducing the transcription of pro-inflammatory cytokines such as TNF-α and IL-6[16]. Additionally, SRC inhibition disrupts TLR4 signaling by interfering with MyD88 and Mal/Tirap recruitment, leading to attenuated MAPK activation and cytokine production. The inhibition of SRC also downregulates p38, ERK, and JNK MAPK pathways, further limiting inflammatory mediator release. Moreover, it reduces integrin β3 and focal adhesion kinase (FAK) activity, thereby suppressing immune cell recruitment and adhesion[17]. Furthermore, SRC inhibition alters SHP-1-Pyk2-SRC signaling, impacting IL-10 production and shifting the immune response toward an anti-inflammatory state[18]. Collectively, these mechanisms highlight SRC as a promising therapeutic target for controlling excessive inflammation in various disease conditions. Thus, SRC was selected for validation due to its critical role in modulating inflammatory responses in macrophages and its high connectivity in the PPI network.

In this study, SRC was selected as the target enzyme for evaluation, with Staurosporine (STS) used as a positive control drug. Based on network pharmacology predictions and previous experimental isolation of hawthorn leaf compounds, three representative triterpenoids (compounds 99, 102, and 116) were selected for SRC kinase inhibition assays. The experimental results are shown in Fig. 4. As depicted in Fig. 4, compounds 99, 102, and 116 demonstrated inhibitory activity against SRC kinase, with inhibition rates positively correlated with concentration. The IC_{50} values for compounds 99, 102, and 116 were 22.46 μM, 26.90 μM, and 29.89 μM, respectively, which were higher than that of the positive control drug, STS. Despite this, the three triterpenoids exhibited significant SRC inhibitory activity, with compound 99 showing the most potent effect.

Molecular docking and molecular dynamics simulations

Molecular docking

Molecular docking was performed to evaluate the interactions between the three core triterpenoid compounds (99, 102, and 116) and the key target protein SRC, based on network pharmacology predictions and results from target enzyme and anti-inflammatory activity experiments. The results are presented in Fig. 5, which includes two-dimensional interaction diagrams and three-dimensional structural models (Figs. 5 A and 5B) to illustrate the compound-SRC interactions. In the two-dimensional interaction diagrams, different interaction types were represented by specific color markers: bright green for van der Waals forces, dark green for hydrogen bonds, and pink for C-H…π or inter-C-H forces.

Compound 99: This compound interacted with multiple SRC amino acid residues, including 18GLY, 88GLY, 89SER, 137LEU, 91LEU, 41LEU, 151LEU, 22PHE, 39LYS, 148 ASP, 166PRO, 20GLY, 132 ARG, and 19GLN via van der Waals forces. Additionally, residues 134 ALA, 17LEU, 25 VAL, and 21 CYS enhanced binding affinity through interalkyl forces.

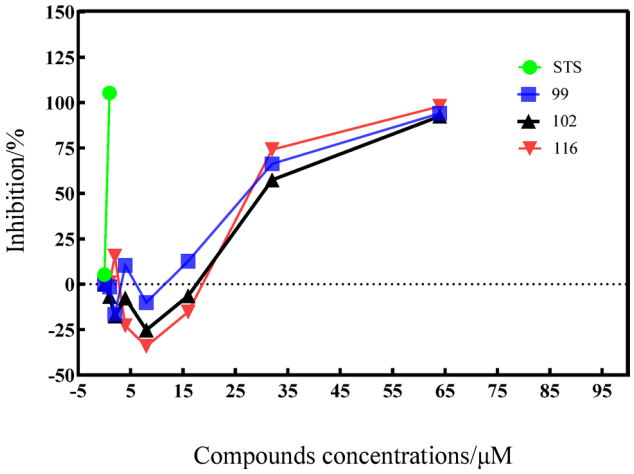

Fig. 4. Inhibitory activity of compounds against SRC kinase.

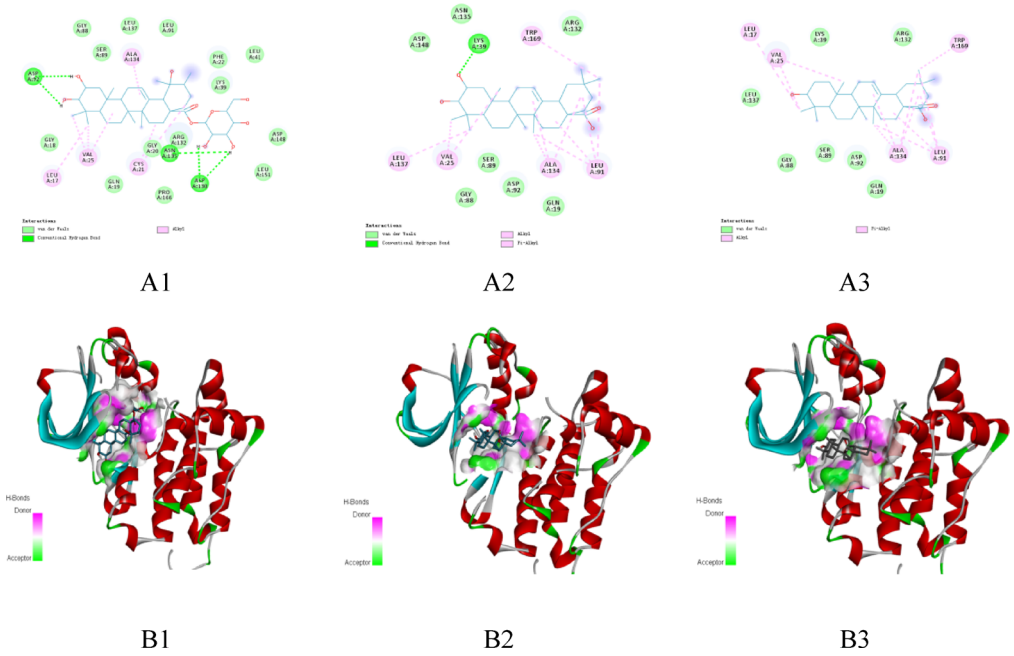

Fig. 5. Molecular docking and visualization. (A1–A3) Two-dimensional (2D) visualizations of the molecular docking interactions between compounds 99, 102, and 116 and the target protein SRC. The diagrams depict the following interaction types: blue represents the compounds, dark green indicates hydrogen bonds, light green represents van der Waals forces, and pink indicates alkyl and π-alkyl interactions. (B1–B3) Three-dimensional (3D) visualizations of the molecular docking results for compounds 99, 102, and 116 with the target protein SRC, highlighting their spatial binding conformations.

Compound 102: It formed hydrogen bonds with 39LYS and interacted with residues 148 ASP, 135 ASN, 132 ARG, 88GLY, 89SER, 92 ASP, and 19GLN via van der Waals forces. Residues 137LEU, 25 VAL, 169 TRP, 134 ALA, and 91LEU strengthened binding via interalkyl forces.

Compound 116: This compound interacted with residues 137LEU, 39LYS, 132 ARG, 88GLY, 89SER, 92 ASP, and 19GLN through van der Waals forces. C-H…π interactions with 17LEU, 25 VAL, 134 ALA, 91LEU, and 169 TRP enhanced its binding affinity.

Molecular docking results revealed binding free energies of −8.4, −7.2, and −7.3 kcal/mol for compounds 99, 102, and 116, respectively. Among the three, compound 99 exhibited the strongest binding affinity for SRC, consistent with the results from kinase inhibition assays and inflammatory cell model experiments. These findings underscore the potent anti-inflammatory activity of compound 99 and its strong binding capability with SRC, highlighting its therapeutic potential.

Molecular dynamics simulations of compound 99 and SRC

To further evaluate the binding affinity and stability between compound 99 and the target protein SRC, 100 ns molecular dynamics (MD) simulations were conducted based on the molecular docking results. The simulations utilized the OPLS-2005 force field, and the results are depicted in Fig. 6.

RMSD Analysis: As shown in Fig. 6A, the root-mean-square deviation (RMSD) curves demonstrate that the protein's RMSD (left Y-axis) stabilized at approximately 1.8 Å, while the ligand's RMSD (right Y-axis) reached stability at around 9 Å. These results indicate good binding stability of compound 99 to SRC throughout the simulation.

RMSF Analysis: Fig. 6B illustrates the root-mean-square fluctuation (RMSF) of SRC amino acid residues during the simulation. Minimal fluctuations were observed, further confirming the structural stability of the SRC-compound 99 complex[19].

Interaction Analysis: The interaction forces and contact frequencies between compound 99 and SRC are presented in Fig. 6C. Hydrogen bonding, hydrophobic interactions, ionic interactions, and water bridges were the categories used for the interactions. The stacked bar graphs reveal frequent and strong contacts between SRC and compound 99, indicating robust and stable binding of the complex. Collectively, these findings demonstrate the strong binding affinity and structural stability of compound 99 to SRC, highlighting its potential as a therapeutic agent.

Experimental validation of models of inflammatory cells

Effects of compounds at different concentrations on RAW264.7 cell viability

The MTT assay, as described in Sect. 2.2.4.1, was used to evaluate the cytotoxic effects of the compounds at different concentrations. Figure 7 shows that RAW264.7 cells were exposed to varying concentrations of the compounds for a 24-hour period. At concentrations below 25 μM, none of the tested compounds exhibited significant cytotoxic effects, with cell viability rates consistently exceeding 80%. These results indicate that the compounds are non-toxic at these concentrations. Consequently, subsequent anti-inflammatory activity studies were conducted using compound concentrations below 25 μM to determine their efficacy in modulating inflammatory responses.

Effect of compounds on NO content in RAW264.7 cells

The anti-inflammatory effects of compounds 99, 102, and 116, and their interactions with the key target protein SRC, were evaluated using an LPS-induced inflammatory cell model. As shown in Fig. 8, LPS stimulation caused a notable increase in nitric oxide (NO) production in RAW264.7 macrophages when compared to the

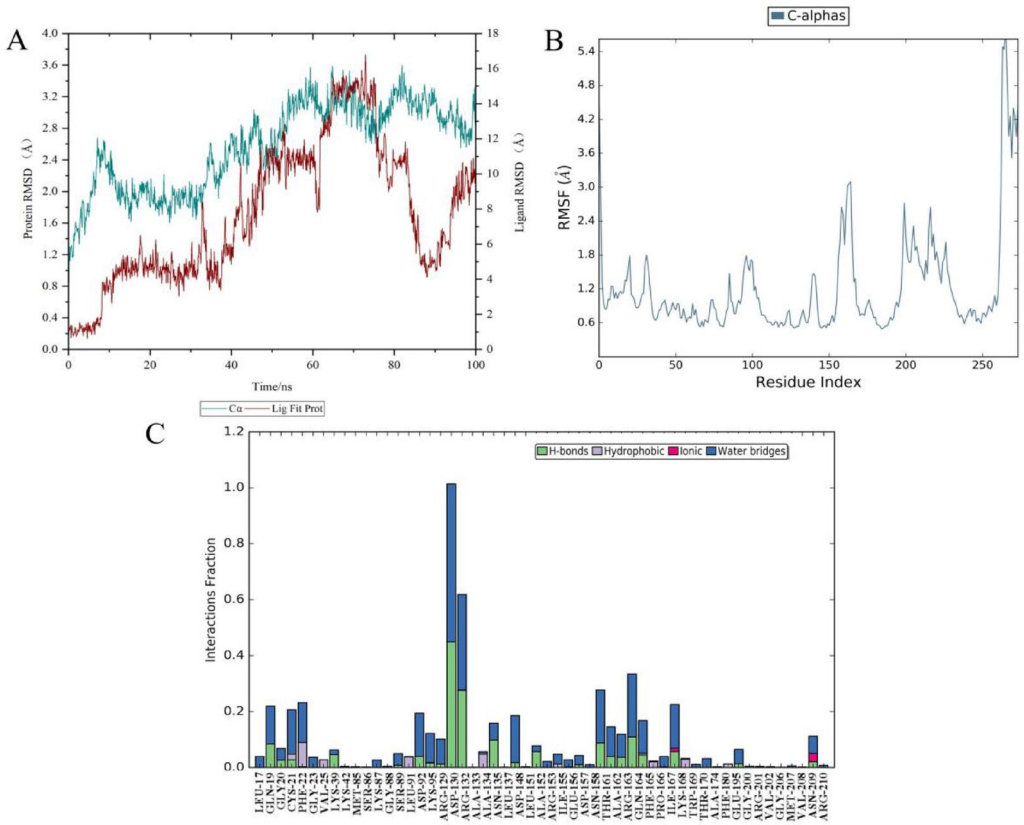

Fig. 6. MD simulation of compound 99 in SRC. (**A**) RMSD curve of compound 99 interacting with SRC. (**B**) RMSF curve of compound 99 interacting with SRC. (**C**) Interaction fraction of compound 99 with SRC.

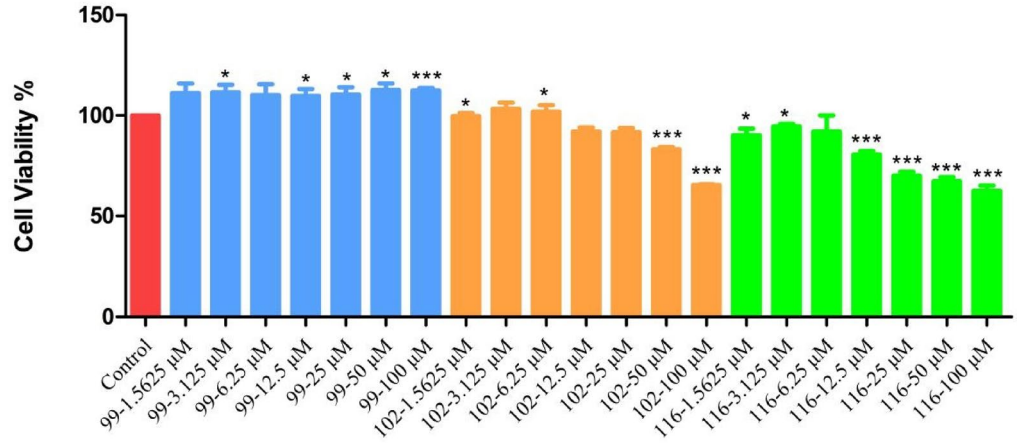

Fig. 7. Effects of compound concentrations on RAW 264.7 cell viability.

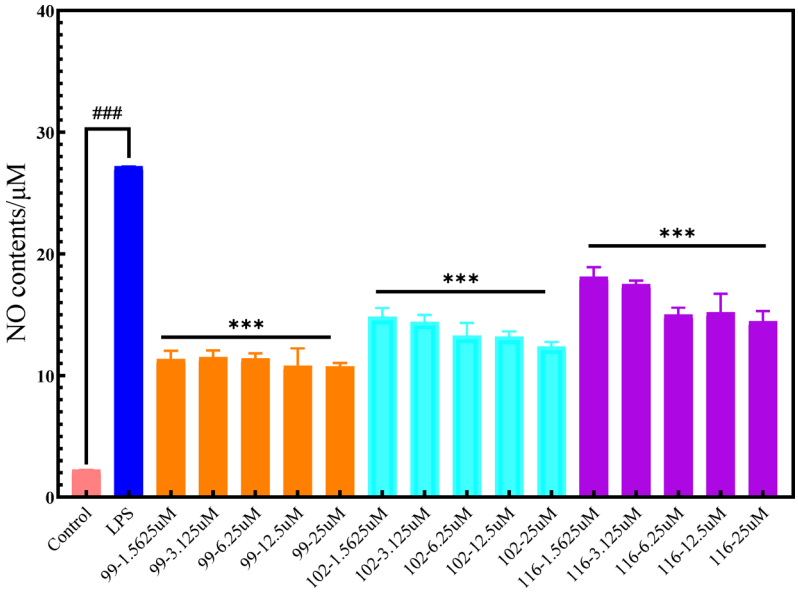

Fig. 8. Effects of compounds on NO content in RAW 264.7 Cells.(x ± s, $n = 3$).$^{\#\#}P < 0.01$, $^{\#\#\#}P < 0.001$ vs. Control group. $^{*}P < 0.05$, $^{**}P < 0.01$, $^{***}P < 0.001$ vs. the model group.

blank control group ($P < 0.001$), verifying the successful creation of the inflammation model. Treatment with compounds 99, 102, and 116 at concentrations of 6.25, 12.5, and 25 μM for 24 h significantly reduced NO production compared to the model group ($P < 0.001$). Among the tested compounds, compound 99 exhibited the strongest inhibitory effect, reducing NO content to 10.74 μM at a concentration of 25 μM ($P < 0.001$). These findings suggest that triterpenoids from hawthorn leaves exert anti-inflammatory effects by markedly inhibiting LPS-induced NO production in RAW264.7 cells.

Real-time fluorescence quantitative qRT-PCR assay

To explore how compound 99 inhibits SRC expression, qRT-PCR was performed to evaluate the expression levels of genes related to SRC. As shown in Fig. 9, treatment with compound 99 at various concentrations significantly reduced SRC mRNA expression compared to the LPS-treated control group ($P < 0.001$). These findings suggest that compound 99 exerts notable anti-inflammatory effects, likely through its ability to downregulate SRC mRNA expression. The results underscore the therapeutic potential of compound 99 as a promising candidate for mitigating inflammation. Future studies are warranted to explore the specific regulatory pathways and gain a deeper understanding of the molecular mechanisms underlying its anti-inflammatory activity.

Western blotting of SRC protein expression

Western blot analysis demonstrated that treatment with the compound 99 markedly suppressed the expression of Src protein. Compared to the model group, cells treated with compound 99 exhibited a significant reduction

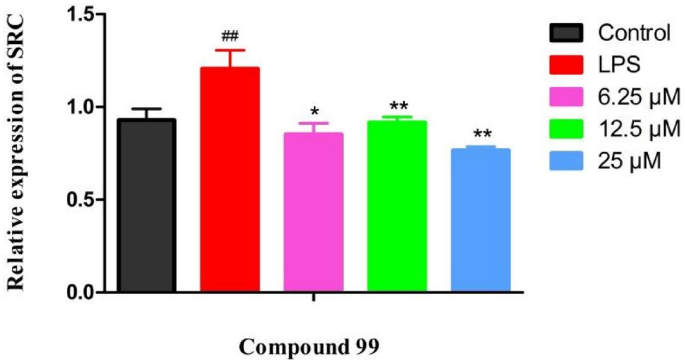

Fig. 9. Effect of compound 99 on SRC mRNA expression levels. Data are expressed as the mean ± SD, $n = 3$. $^{\#\#}P < 0.01$, $^{\#\#\#}P < 0.001$ vs. Control group. $^{*}P < 0.05$, $^{**}P < 0.01$, $^{***}P < 0.001$ vs. the model group.

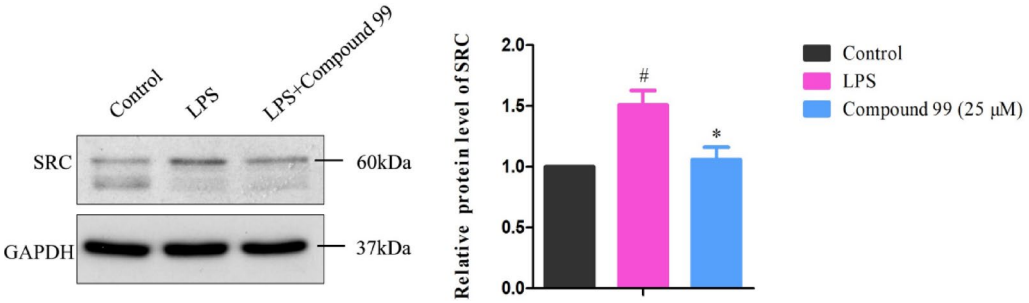

Fig. 10. Western blotting of SRC protein expression. Data was expressed as the mean ± SD, $n = 3$. $^{*}P < 0.05$ vs. the model group, $^{\#}P < 0.05$ vs. Control group.

in Src protein levels ($P < 0.05$), while GAPDH levels remained unchanged across all groups, confirming equal protein loading (Fig. 10). These findings suggest that the compound 99 effectively downregulates Src protein expression, which may contribute to its pharmacological mechanism of action.

Conclusions

Network pharmacology was applied to identify the key chemical compounds, core targets, and signaling pathways that contribute to the anti-inflammatory effects of hawthorn leaves. Experimental validation confirmed that triterpenoids 99, 102, and 116 exhibited strong binding affinities for SRC kinase and effectively inhibited nitric oxide (NO) release in macrophages. Among these compounds, triterpenoid 99 exhibited the most potent anti-inflammatory activity by modulating SRC mRNA and protein expression, reducing the secretion of inflammatory mediators, thereby regulating the initiation and progression of inflammation. The study provides a robust theoretical basis for the medicinal application of hawthorn leaves and offers a promising strategy for the development of novel treatments targeting severe inflammation.

Materials and methods

Experimental materials

The Hawthorn leaf was procured from China Golden Herb Traditional Chinese Medicine Drinking Tablets Co., Ltd. and was authenticated by Professor Guang-shu Wang of Jilin University as the dried leaf of *Crataegus pinnatifida* Bge., belonging to the family *Rosaceae*. The author's group isolated and purified Compound 99 to about 85% purity, while Compounds 102 and 116 were purchased as controls with approximately 95% purity; Phosphoric acid (analytical reagent-grade, Merck, Germany), dimethyl sulfoxide (Solarbio); SRC, (N-2-hydroxyethylpiperazine-N-2-ethane sulfonic acid) HEPES (Carna Biosciences); EDTA (Thermo Fisher Scientific Inc.); (dithiothreitol) DTT (Sigma); p-aminobenzenesulfonic acid, naphthalene ethylenediamine hydrochloride, lipopolysaccharides (Shanghai Macklin Biochemical Co., Ltd.); total NOS inhibitor (Beyotime Biotechnology Co., Ltd.); Macrophage RAW 264.7 was purchased from Cell Bank of the Typical Cultures Preservation Committee of the Chinese Academy of Sciences; PBS, MEM medium, penicillin/streptomycin solution (Dalian Meilun Biotechnology Co., Ltd.). The primary antibody used for detecting SRC was the Src (PTR 2316) Mouse mAb, purchased from ImmunoWay Company (Catalog No.: YM4271). Other reagents were all of analytical grade. Enzyme labeling instrument (Berthold Mithras2 LB 943, Germany); Micro nucleic acid protein quantifier (Qubit3.0, Thermo Fisher Scientific Inc).

Experimental methods

Network pharmacology to predict the mechanism of action of hawthorn leaf

Firstly, 116 chemical compounds in hawthorn leaves were established using the TCMSP database. Then, potential targets related the compounds of hawthorn leaves were predicted through the Pharm Mapper online server. The official gene names were verified, and duplicate targets were removed using the Uni Prot database (https://www.uniprot.org/uniprotkb/). Targets associated with inflammation were found using the Gene Cards database (https://www.genecards.org/) by searching the keyword "inflammation", and only human (Homo sapiens) targets were kept after integration and removal of duplicates.

To identify intersection targets, inflammation-related targets were cross-referenced with hawthorn leaf compound targets using Venny 2.1 to generate a Venn diagram. The intersection targets were then imported into the STRING database to explore protein-protein interactions (PPI). Analysis was conducted in "multiple proteins" mode with the organism set to Homo sapiens and a confidence score threshold of 0.900. The PPI network was constructed, and core targets were identified based on their connectivity within the network. The relationships between active compounds and their targets were visualized using Cytoscape software, where nodes represented compounds or targets, and edges denoted interactions, highlighting the complex associations between hawthorn leaf constituents and inflammation-related targets.

Functional annotation of the identified targets was performed using the DAVID database (https://davidbioinformatics.nih.gov/), including Gene Ontology (GO) and KEGG pathway enrichment analyses. The GO analysis included three categories: biological processes (BP), cellular components (CC), and molecular functions (MF). KEGG pathway enrichment showed that these targets are involved in signaling pathways related to inflammation, providing deeper insights into the molecular mechanisms of hawthorn leaf compounds.

Experimental validation of target enzyme

Based on the network pharmacology predictions, SRC was selected as the target enzyme for experimental validation. Staurosporine (STS) served as the positive control drug. Representative triterpenoids (compounds 99, 102, and 116) isolated from hawthorn leaves during preliminary experiments were used in the experimental group. The activity validation experiments were conducted by Shanghai Rui Zhi Pharmaceutical Group Co. Ltd. using a mobility shift assay method. The experimental procedure was as follows.

Preparation of solutions Kinase buffer: 50 mmol/L HEPES (pH 7.5), 0.005% Brij-35, 2 mmol/L DTT, 10 mmol/L $MgCl_2$. Stop solution: 100 mmol/L HEPES (pH 7.5), 0.015% Brij-35, 0.2% Coating Reagent #3, 50 mmol/L EDTA.

Compound preparation The test compounds were prepared as 10 mmol/L stock solutions in DMSO and diluted to 2560 μmol/L. A volume of 100 μL of the diluted compounds was added to a 96-well plate and further subjected to gradient dilution. For the assay, 10 μL of each diluted compound was mixed with 10 μL of DMSO and 90 μL of 1× kinase buffer in the assay plate.

Enzyme and substrate preparation A 2.5× enzyme solution was prepared by diluting SRC kinase into the 1× kinase buffer. A 2.5× peptide solution, containing FAM-labeled peptide, ATP, and $MgCl_2$ in 1× kinase buffer, was also prepared.

Assay procedure Each well received 10 μL of the 2.5× enzyme solution, which was then incubated at room temperature for 10 min. After incubation, 10 μL of the 2.5× peptide solution was added to start the reaction. The reaction was carried out for 30 min at 28 °C and terminated by adding 25 μL of the stop solution to each well.

Data analysis The conversion values of all samples were measured using an EZ Reader II system (Caliper Life Sciences, Waltham, MA, USA) under the following parameters: downstream voltage − 500 V, upstream voltage − 2250 V, base pressure − 0.5 PSI, screen pressure − 1.2 PSI. The percentage inhibition was calculated using the following Eq[20].:

$$Inhibition\ (\%) = [(C_{max} - C_{conversion}) / (C_{max} - C_{min})] \times 100 \quad (1)$$

Where:

C_{max}: Conversion value of the DMSO control.

C_{min}: Conversion value of the enzyme-free control.

$C_{conversion}$: Conversion value at the specified compound concentration.

Validation of molecular docking and molecular dynamics simulations

Molecular docking was conducted using Auto Dock Vina software. The target protein structures were retrieved from the Protein Data Bank (PDB, https://www.rcsb.org/), with water molecules and ligands removed to prepare the proteins for docking. Lower docking scores indicated stronger receptor-ligand affinities and more stable binding conformations[21,22]. Binding energies below − 5 kcal/mol were considered indicative of favorable interactions between the compounds and target proteins, and the docking results were visualized to confirm these interactions.

To further evaluate the binding strength and stability of the compound-protein complexes, molecular dynamics simulations were performed using Schrödinger software. The complex formed by compound 99 and SRC, which exhibited the best docking results, was simulated for 100 ns. The Amber14 sb and GAFF2 force fields were applied to the protein and ligand, respectively. Simulation trajectories were analyzed using metrics such

as root mean square deviation (RMSD) and root mean square fluctuation (RMSF). Additionally, the frequency and duration of key interactions, such as hydrogen bonding, were examined to provide deeper insights into the stability of the compound-protein complex.

Validation of the RAW264.7 cellular inflammation model in vitro

Compound cytotoxicity assay Macrophage RAW 264.7 was purchased from Cell Bank of the Typical Cultures Preservation Committee of the Chinese Academy of Sciences. RAW264.7 cells in the log phase of growth were counted with a cell counting plate and placed into 96-well plates at a concentration of 2×10^4 cells per well. They were then incubated at 37 °C with 5% CO_2 for 24 h. Following incubation, the supernatant was discarded, and sample solutions of varying concentrations (1.5625 μM, 3.125 μM, 6.25 μM, 12.5 μM, 25.0 μM, 50.0 μM, and 100 μM) prepared in culture medium were added to the wells. A blank group received 100 μL of culture medium without any treatment. The cells were further incubated for 24 h under the same conditions. Subsequently, 20 μL of MTT solution (5 mg/mL) was added to each well, and the plates were incubated for 3.5 h at 37 °C in the dark. The supernatant was carefully removed, and 150 μL of DMSO was added to each well to dissolve the formazan crystals. The plates were gently shaken for 10 min, and the absorbance was measured at 490 nm using a microplate reader[23]. The assay was conducted in triplicate, and the average absorbance was calculated for analysis. Cell viability (%) was determined using the following formula:

$$Cell\ survival\ rate\ = A_{sample}/A_{blank} \times 100 \quad (2)$$

Where: A_{sample} is the absorbance of the sample, and A_{blank} is the absorbance of the blank group.

Effect of compounds on NO levels in RAW264.7 cells Standard Curve Determination: To construct a standard curve for nitric oxide (NO) quantification, a series of $NaNO_2$ solutions with concentrations of 0, 1, 2, 5, 10, 20, 40, 60, and 100 μM were prepared. Each concentration was added to a 96-well plate in triplicate. Subsequently, 50 μL of Griess Reagent I was added to each well at room temperature, followed by an equal volume of Griess Reagent II under the same conditions. The plate was left undisturbed for 5 min to enable color formation, and the absorbance of each well was measured at 540 nm with a microplate reader. The standard curve was generated based on the absorbance values and is represented by the following equation:

$y = 0.0071x + 0.2691$ (3), with a correlation coefficient (R) of 0.9958, where y represents absorbance and x indicates NO content (μM).

Effect of Compounds on NO Production: RAW264.7 cells in the logarithmic growth phase were seeded into 96-well plates at a density of 2×10^4 cells per well and incubated at 37 °C with 5% CO_2 for 24 h. After discarding the culture medium, the cells were treated with varying concentrations of compound solutions (1.5625, 3.125, 6.25, 12.5, and 25 μM) in 50 μL of medium per well. The blank and inflammation control groups received 50 μL of culture medium. After 4 h of incubation, 50 μL of LPS solution (0.5 μg/mL) was added to the inflammation and sample groups, while the blank group received an equal volume of culture medium. Following 24 h of further incubation, the absorbance at 540 nm was measured to quantify the NO content using a microplate reader. Each measurement was performed in triplicate, and the average absorbance was calculated for analysis[24]. The NO concentration in the samples was determined using the standard curve equation y=0.0071x+0.2691.

Quantitative real-time PCR (qRT-PCR) analysis

RAW264.7 cells were placed in 6-well plates at a concentration of 3×10^5 cells per well and exposed to sample solutions at 6.25, 12.5, and 25 μM for 2 h. Subsequently, 0.5 μg/mL of LPS solution was added to the sample and inflammation groups, while the blank group received culture medium alone. After 24 h of incubation, the cells were washed three times with phosphate-buffered saline (PBS) and lysed with a cell lysis buffer. Total RNA was extracted using a total RNA extraction kit, and RNA purity and concentration were measured using a UV spectrophotometer. cDNA was synthesized via reverse transcription using the TaKaRa RT kit, and quantitative real-time PCR (qRT-PCR) was performed using TB Green Premix Ex Taq II (RR420Q, Takara Bio Inc., Japan). The reaction conditions were as follows: 50 °C for 2 min (initial step), 95 °C for 10 min (pre-denaturation), followed by 40 cycles of 95 °C for 15 s (denaturation) and 60 °C for 40 s (annealing). Fluorescence detection was performed at the end of each cycle.The experiments were conducted in triplicate, and the results were analyzed using the ΔΔCT method[25]. qRT-PCR detection of the compounds was entrusted to Oden Biotechnology (Shenyang) Co., Ltd.

Western blot analysis

To investigate the underlying molecular mechanism, Western blotting was performed as previously described[26]. RAW264.7 cells were cultured under identical conditions to those mentioned above. Cell pellets were lysed in RIPA buffer supplemented with PMSF at a ratio of 100:1, followed by thorough mixing. After centrifugation at 12,000 rpm for 20 min, the supernatants containing total protein were collected. Equal amounts of protein (10 μg per lane) were subjected to electrophoresis on 12% SDS-PAGE gels and subsequently transferred onto PVDF membranes (0.45 μm pore size). The membranes were then blocked for 1 h and incubated overnight at 4 °C with primary antibodies targeting SRC (1:500) and GAPDH (1:1000). This was followed by a 2 h incubation with HRP-conjugated secondary antibodies (1:5000) at room temperature. Protein bands were visualized using an enhanced chemiluminescence detection system (Tanon 5500, China).

Statistical analysis

All data analysis was conducted with GraphPad Prism 9.0 software. Comparisons across multiple groups utilized one-way ANOVA. The determination of statistical significance was based on these P-value thresholds: P-values

below 0.05 were marked as statistically significant, below 0.01 as very significant, and below 0.001 as highly significant.

Data availability

Data is provided within the manuscript or supplementary information files.The original contributions presented in the study are included in the article, further inquiries can be directed to the corresponding author.

Received: 4 February 2025; Accepted: 3 June 2025
Published online: 01 July 2025

References

1. Gennaro, C., Marco, A., & Morena, T. L. Periodontitis, Low-Grade inflammation and systemic health: A scoping review. *Med. (Kaunas)*. **56**, 272 (2020).
2. Gowd, V. et al. Role of sam68 as an adaptor protein in inflammatory signaling. *Cell. Mol. Life Sci.* **81**, 89–91 (2024).
3. Diego, C. The role of gut microbiota in the modulation of drug action: a focus on some clinically significant issues. *Expert Rev. Clin. Pharmacol.* **11**, 171–183 (2018).
4. Kyungseop, A. The worldwide trend of using botanical drugs and strategies for developing global drugs. *BMB Rep.* **50**, 111–116 (2017).
5. Li, T. et al. Biological properties and potential application of Hawthorn and its major functional components: A review. *J. Funct. Foods*. **9**, 104988 (2022).
6. Liu, X. G. et al. Mechanism of action of Hawthorn leaves against hyperlipidemia based on network Pharmacology and preliminary validation study. *Sci. Technol. Food Ind.* **43**, 36–45 (2022).
7. Abolfazl, A. et al. Physicochemical Characterization,Antioxidant Activity, and Phenolic Compounds of Hawthorn (Crataegus spp.) Fruits Species for Potential Use in Food Applications. *Foods*. **9**, 436 (2020).
8. Quan, Y. C., Guan, L. P. Anti-inflammatory, analgesic effects of Hawthorn leaf extracts. *Lishizhen Med. Mater. Med. Res.* **17**, 556–557 (2006).
9. Sun, Z. et al. Vitexin attenuates acute doxorubicin cardiotoxicity in rats via the suppression of oxidative stress, inflammation and apoptosis and the activation of FOXO3a. *Exp. Ther. Med.* **12**, 1879–1884 (2016).
10. Min, Q. et al. Hawthorn leaf flavonoids protect against Diabetes-Induced cardiomyopathy in rats via PKC-α signaling pathway. *Evid. Based Complement. Alternat. Med.* **2017**, 2071952 (2017).
11. Nascimento, R. P. D. et al. Chemoprevention with a tea from hawthorn (Crataegus oxyacantha) leaves and flowers attenuates colitis in rats by reducing inflammation and oxidative stress. *Food Chem. X* **12**, 100139 (2021).
12. Yue, C. X. et al. Maslinic acid protects against LPS-induced inflammatory response in RAW264.7 cells by regulating phosphorylation of STAT3. *Food Mach.* **37**, 36–42 (2021).
13. Li, R. Y. et al. Crataegus pinnatifida: A botanical, ethnopharmacological, phytochemical, and Pharmacological overview. *J. Ethnopharmacol.* **301**, 115819 (2023).
14. Yap, H. W., Lim, Y. M. Mechanistic Perspectives of Maslinic Acid in Targeting Inflammation. *Biochem. Res. Int.* **2015**, 279356 (2015).
15. Cai, Y. X., Xu, J., & Cheng, Q. H. Proto-oncogene tyrosine-protein kinase SRC (Src) Inhibition in microglia relieves neuroinflammation in neuropathic pain mouse models. *Bioengineered* **12**, 11390–11398 (2021).
16. Lee, H. S. et al. Src tyrosine kinases mediate activations of NF-κB and integrin signal during lipopolysaccharide-induced acute lung injury. *J. Immunol.* **179**, 7001–7011 (2007).
17. Jonathon, M. et al. Src family kinase tyrosine phosphorylates Toll-like receptor 4 to dissociate MyD88 and mal/tirap suppressing LPS-induced inflammatory responses. *Biochem Pharmacol.* **147**, 119-127 (2018).
18. Okenwa, C. et al. SHP-1–Pyk2–Src protein complex and p38 MAPK pathways independently regulate IL-10 production in lipopolysaccharide-stimulated macrophages. *J. Immunol.* **191**, 2589-2603 (2013).
19. Chen, S. et al. Exploring the molecular mechanism of Shuangjiang Weitong pill in the treatment of gastritis based on network pharmacology, molecular Docking and molecular dynamics simulations. *J. Yunnan Univ. Chin. Med.* **47**, 57–71 (2024).
20. Salvatore, D. M. et al. Applying molecular hybridization to design a new class of pyrazolo[3,4-d]pyrimidines as Src inhibitors active in hepatocellular carcinoma. *Eur. J. Med. Chem.* **280**, 116929 (2024).
21. Song, L. Y., Li, L. H. & Bi S. T. Study on the mechanism of *Astragali Radix* extract in treating hypoxic-ischemic encephalopathy based on network pharmacology, molecular Docking and experimental validation. *Nat. Prod. Res. Dev.* **36**, 520–527 (2024).
22. Ye, J. R. et al. Mechanism of active ingredients from *Scutellaria radix* on alcoholic liver disease based on network Pharmacology and molecular Docking and effect verification. *Nat. Prod. Res. Dev.* **35**, 1602–1612 (2023).
23. Mosmann, T. Rapid colorimetric assay for cellular growth and survival: application to proliferation and cytotoxicity assays. *J. Immunol. Methods*. **65**, 55–63 (1983).
24. Fan, Y. Q. et al. Terpenoids from *Fructus Leonuri* and their anti-inflammatory activities. *Chin. Pharm. J.* **58**, 571–575 (2023).
25. Lin, H. et al. EF24 induces ferroptosis in osteosarcoma cells through HMOX1. *Biomed. Pharmacother.* **136**, 111202 (2021).
26. Zeng, X. Z. et al. Aconine inhibits RANKL-induced osteoclast differentiation in RAW264.7 cells by suppressing NF-κB and NFATc1 activation and DC-STAMP expression. *Acta Pharmacol. Sin.* **37** (2), 255–263 (2016).

Acknowledgements

Authors sincerely acknowledge Prof. Jian Wang of Shenyang Pharmaceutical University for technical support of Desmond Module of Schrodinger. his research was funded by the Science and Technology Development Program of Jilin Province (No. 20210402038GH).

Author contributions

Conceptualization, data curation, and writing—original draft, Zhixing LIU; writing—review and editing, supervision, funding acquisition, Jihua LIU.

Declarations

Competing interests

The authors declare no competing interests.

Additional information

Supplementary Information The online version contains supplementary material available at https://doi.org/10.1038/s41598-025-05573-1.

Correspondence and requests for materials should be addressed to J.L.

Reprints and permissions information is available at www.nature.com/reprints.

Publisher's note Springer Nature remains neutral with regard to jurisdictional claims in published maps and institutional affiliations.